Available online at www.sciencedirect.com

ScienceDirect

Procedia Computer Science 00 (2023) 000–000

Procedia Computer Science

www.elsevier.com/locate/procedia

The 14th International Conference on Ambient Systems, Networks and Technologies (ANT)
March 15-17, 2023, Leuven, Belgium

Waiting Time Analysis for a Network of Signalized Intersections

Radha Reddy[a,b,c,*], Luis Almeida[a,c], Pedro Santos[a,b,c], Eduardo Tovar[a,b]

[a] *CISTER Research Centre, Rua Alfredo Allen, 535, 4200-135 Porto, Portugal*
[b] *Instituto Superior de Engenharia do Porto (ISEP), R. Dr. António Bernardino de Almeida 431, 4200-135 Porto, Portugal*
[c] *FEUP, University of Porto, R. Dr. Roberto Frias, 4200-465 Porto, Portugal*

Abstract

Vehicle waiting time or stopped delay is one of the major disadvantages of employing signalized intersections (SIs) in road networks. The waiting time delays occur when vehicles stop in the queue, waiting to access the SI, and vary from road lane to road lane with the intersection management (IM) protocol used. In this research line, we propose an analytical expression for estimating the waiting time delays and studying the performance of different IM approaches in a grid network of independent intersections. We consider complex intersections with four legs and two lanes with two left-lane configurations, as well as five state-of-the-art IM approaches: two conventional – Round-Robin (RR) and Trivial Traffic Light Control (TTLC); two adaptive – Max-pressure Control Algorithm (MCA) and Websters Traffic Light Control (WTLC); and one reactive – Synchronous Intersection Management Protocol (SIMP). The waiting time performance of these five IM approaches is compared using two simulation scenarios in the SUMO simulation framework. The simulation results validate the analytical study and show the advantages of employing SIMP, being the IM approach with the lowest waiting time delays.

Keywords: Efficient intersections; Stopped delay or waiting time delay; Road network of intersections; Synchronous intelligent intersections.

1. Introduction

Over the years, private vehicles have been the growing means of transportation in urban areas, leading to congestion, particularly at signalized intersections (SIs). Numerous intersection management (IM) approaches were designed to manage SIs and mitigate traffic congestion [8]. IM approaches can be classified based on their working nature from conventional, which operates with a fixed cycle [1, 2], to intelligent, which adapts cycle times based on inflow traffic properties [3, 4], cooperative, that coordinates to improve a global metric [5], and reactive, that use fine-grain cycles for quick reaction to actual traffic [6, 7]. The effectiveness of the IM approaches can be measured by travel time, speed, delays, queue length, number of stops, density, and travel-time variance [9]. According to Olszewski [10], vehicles stop delay (or waiting time delay) is one of the most common performance metrics of SIs, as it indicates the disruption caused by the IM operations and the traffic congestion. Moreover, the work of [11] established the relationship

* Corresponding author.
E-mail address: reddy@isep.ipp.pt

between perceived waiting time (user's knowledge about the waiting time) and the level of service of SIs, while [13] compared the user perceived and virtually surveyed waiting time values through driving simulation.

In this work, we also study the waiting time performance of IM approaches, focusing on a network of independent SIs, i.e., intersections operate independently without any cooperation or coordination among them. Each SI is complex, with four legs and two lanes. The right lane serves traffic turning right and going straight while the left lane has two configurations: dedicated - serves traffic turning left, or shared - serves traffic turning left and going straight [15]. We use five state-of-the-art IM approaches for managing the intersections. Among the five, two are conventional (Round-Robin - RR and Trivial Traffic Light Control - TTLC [1]), two are adaptive (Max-pressure Control Algorithm - MCA [3] and Websters Traffic Light Control - WTLC [4]), and one is reactive (Synchronous Intersection Management Protocol - SIMP [7]).

Firstly, we present an analytical model for estimating the maximum waiting time delays in a small grid network with 2×2 SIs using road lane capacity, traffic flow information, and IM-specific parameters, such as queue length, green phase time, traffic light control (TLC) cycle length, and the maximum number of vehicles that can be served in a green phase. This analysis can be applied to different road networks with small adaptations, but its generalization to arbitrary networks of SIs is left for future work. Secondly, we validate the analytical results with simulated experimental scenarios using the SUMO simulation framework [16]. The results show the dominance of SIMP against its counterparts in the tested scenarios exhibiting the lowest waiting time values and the smallest difference between the analytical and observed results.

2. Related Work

Numerous IM approaches can be found in the literature for traffic management, congestion mitigation, and delay minimization, some specifically aiming at traffic with Autonomous Vehicles (AVs) only, others being agnostic to the specific features of AVs and aiming at mixed traffic with AVs and Human-driven Vehicles (HVs). For instance, conventional approaches (RR and TTLC [1]) are introduced to simply manage the traffic and avoid collisions at individual intersections. They operate for a fixed green phase time switching between lanes cyclically. Boon and Van [2] presented an algorithmic methodology for decomposing a network of intersections and managing each intersection with fixed cycles. On the contrary, MCA operates for a fixed minimum green phase time acyclically and adapts the green phase length dynamically depending on traffic flow movement [3]. Other approaches, like WTLC, adapt their green phase time between the minimum and maximum TLC cycle lengths using the traffic flow data [4]. In other cases [5], the cycles of the intersections are synchronized and the green phases shift as necessary so that the vehicles from different lanes cross the intersection alternatively without stopping. Differently, SIMP protocol synchronizes the vehicles movements in very short cycles, corresponding to one vehicle crossing at a time from each non-conflicting road lane [6, 7]. The work in [8] discusses IM approaches from a multi-dimensional perspective, including road network type, priority, and supporting strategy, with objectives (delays, throughput, etc.) and constraints (cycle length, green time, etc.). Most of these approaches use simulation-based waiting time delays.

A few research works, only, explicitly studied waiting time delays at SIs. For instance, Olszewski [10] presented an extensive theoretical analysis in which the relation between the overall and stopped delays is drawn respecting the arrival of platoons. Wu et al. [13] presented the perceived waiting time using the virtual experience survey at an arterial with three SIs. Othayoth and Rao [11] focused on establishing the relationship between perceived waiting time and service levels respecting the SIs of India. They suggested the achieved thresholds to the Indian version of the Highway Capacity Manual (HCM) [12].

Overall, waiting time delays at SIs are observed through simulation studies or surveys. Differently, we employ the IM-specific parameters, along with the road capacity and traffic inflow information, for modeling the analytical expression of maximum waiting time delays and then comparing the analytical against the simulation results.

3. Road Network Architecture

Figure 1a illustrates the road network with a grid of $M \times M$ (with $M = 2$) intersections spanning over a squared area of $D \times D$. The distance between neighboring intersections is given by $l = \frac{D}{M+1}$. Four cardinal directions (n, e, s, w) indicate four sides of the grid network. Each side of the grid connects the external road system through M roads to M intersections. In our case ($M = 2$), the grid north side connects n_1 and n_2 roads with I_0 and I_1 intersections. Similarly, the set of intersections and outer roads of the grid network are $\mathcal{I} = \{I_0, I_1, I_2, I_3\}$ and $\mathcal{O} = \{w_2, n_1, n_2, e_1, e_2, s_1, s_2, w_1\}$,

respectively. All intersections are equipped with an IM unit for implementing the IM protocols and associated control signals for managing traffic inflows (Fig. 1a).

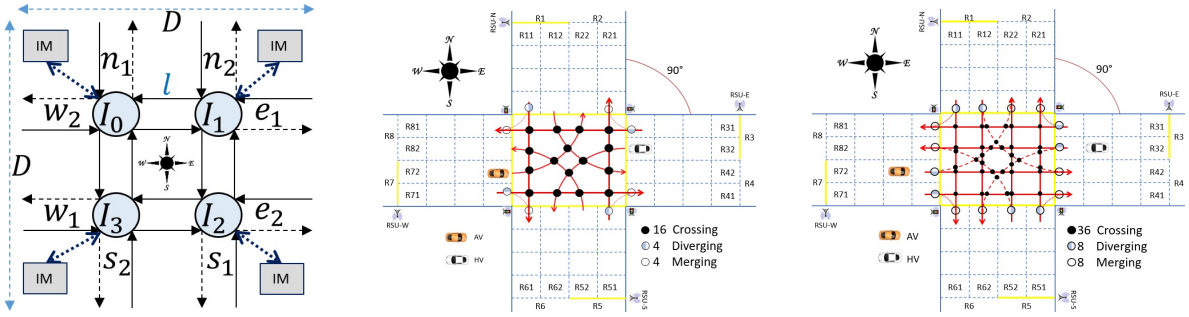

(a) Network of 2×2 intersections. (b) Dedicated left-lane intersection. (c) Shared left-lane intersection.

Fig. 1: Network of intersections and intersection crossing configurations and their conflicts (crossing, diverging, and merging).

The grid network represents a symmetric directed graph in which the directed edges (road lanes) appear twice, one in each direction from vertices (intersections). Also, each road is associated with a degree denoting the number of lanes in either inflow or outflow directions. In our case, we have an edge degree of two (Fig. 1b and 1c).

Figures 1b and 1c depict two typical intersection crossing configurations (dedicated and shared left lanes) of a four-way two-lane road intersection along with the possible conflicts (crossing, diverging, and merging) [15]. Crossing conflicts occur when the vehicles of all inflow lanes want to cross the same intersection location (black dots). We employ these crossing configurations for designing the most suitable TLC phases, which will be used by the IM approaches based on their logic to permit vehicles into the intersection. The diverging conflicts occur when the consecutive vehicles of a single road lane turn to different lanes (half-grey dots). Finally, merging conflicts occur when vehicles from different lanes want to access the same outflow lane (uncolored dots). When we compare the total number of conflicts, the shared left lane intersection has more than that of the dedicated left lane intersection, making the shared left lane more complex to manage than the dedicated left lane configuration.

In Figures 1b and 1c, the 90° angled road lanes (R_{ij} for $i = 1, ..., 8$ and $j = 1, 2$) are indexed with odd (inflow) and even (outflow) numbers. Here, for $i = 1$, $j = 1$ indicates the outermost lane that accommodates straight/right (S/R) crossing traffic and $j = 2$ indicates the centermost lane that accommodates left (L) or left/straight (L/S) crossing traffic. For the sake of simplicity, we use L for both dedicated and shared left-crossing lanes unless otherwise specified. In Figures 1b and 1c, the virtually formed road cells represent the space taken by one vehicle and the safety distance to the following one. We define the road capacity $C(R_{ij})$ for any inflow road lane R_{ij} as the maximum number of vehicles that can be accommodated in the road length. For example, considering a road length of $500m$, a vehicle length of $5m$ and a safety distance of $5m$, we obtain $C = 50$ vehicles. Each road is equipped with road and camera sensors and roadside units (RSUs) for providing appropriate inputs to the intelligent and adaptive IM approaches.

4. Comparing Traffic Light Control Algorithms

Here we introduce the five IM approaches under consideration, i.e., RR, TTLC, MCA, WTLC and SIMP. For fairness, we permit vehicles from non-conflicting right crossing lanes to access the intersections for all IM approaches. Also note that in all protocols but SIMP, a short yellow phase of $4s$ always follows green phases.

Round-Robin (RR) IM, also called Uniform TLC, works in cycles with equally allocated fixed green phase time to all road lanes. RR is cyclic and the green phases rotate through all roads (we consider a clockwise rotation $n - e - s - w - n$). Thus, the total cycle length is fixed.

Trivial Traffic Light Control (TTLC) also operates in cycles using fixed green phases leading to a fixed cycle length [1]. Conversely to RR, TTLC permits vehicles from opposite road lanes, i.e., $n - s$ or $e - w$. The cycle comprises four phases, $n - s$ S/R lanes, $n - s$ L lanes, $e - w$ S/R lanes and finally, $e - w$ L lanes.

Max-pressure Control Algorithm (MCA) is an adaptive acyclic approach with a fixed minimum green phase time [3]. The green phase time adaptation depends on the traffic flow movement, and the lane with the highest movement gets a more prolonged green phase, while the other lanes are blocked with red signals. Like RR, MCA also permits vehicles from one road at a time (green phase).

Websters Traffic Light Control (WTLC) is another adaptive IM approach, using fixed minimum and maximum cycle times [4]. The green phase time adapts based on the traffic flow data obtained by road sensors and the user-specified time interval to adapt. Low time intervals may cause oscillation between consecutive cycles. Like RR, WTLC permits vehicles from a single inflow road at a time and rotates the green phases clockwise.

Synchronous Intersection Management Protocol (SIMP) [6, 7] uses road and camera sensors to detect vehicles at the entrance of the intersection and their desired crossing directions. Other sensors detect vehicles exiting the intersection. This information is also obtained by V2I communication if the vehicles support it for improved robustness. With this information, SIMP serves one vehicle from each lane in sequence but allows one vehicle simultaneously from all other non-conflicting lanes. The next lane is served when all vehicles admitted when serving the previous lane exit the intersection. This synchronizes the access to the intersection from all lanes, vehicle by vehicle. A *conflicting directions matrix* (CDM) is used to decide which vehicles at the intersection entrance are allowed to enter together with the vehicle in the current lane in the cycle. The CDM is designed based on the crossing conflicts shown in Figures 1b and 1c and covers all possible crossing conflicts for vehicles safe passage. Therefore, SIMP is reactive in the sense that a lane is only served if it has a vehicle ready to enter the intersection, or else the next lane is immediately checked. Thus, SIMP is the IM with the shortest cycle length for serving one vehicle from each road lane.

Table 1 summarizes the properties and configurations of these IM approaches employed in this paper, including the green and yellow time per crossing lane (S/R and L), the number of vehicles served during the green phase, and the total cycle time. Note that the MCA is acyclic in nature but, for simplicity, we also present a cycle time, marked with $*$ in Table 1, since the minimum green phase time is known.

Table 1: Summary of the IM approaches under comparison.

IM	Road Infrastructure	Type	S/R - ϕ_g (s)	Yellow (s)	$D_{IM_{i1}}$ (Veh)	L - ϕ_g (s)	Yellow (s)	$D_{IM_{i2}}$ (Veh)	TLC cycle time (s)
RR	No	Fixed	30	4	12	30	4	12	136
TTLC	No	Fixed	30	4	12	15	4	6	106
MCA	Yes	Adaptive	Min-30	4	12	Min-30	4	12	136*
WTLC	Yes	Adaptive	[30 41]	4	[12 16]	[30 41]	4	[12 16]	[136 180]
SIMP	Yes	Reactive	2.5	0	1	3	0	1	11

5. Waiting Time at Signalized Intersections

Here we analyze the specific case of the 2×2 grid network of SIs (Fig. 1a). We focus on the external lanes only, i.e., those receiving traffic from outside the grid or output traffic from the grid. Since our target is to compare different IM approaches used in the SIs, we will keep the traffic balanced on all edges (lanes connecting SIs) to avoid bias caused by specific traffic patterns. We achieve this by fixing the routes for all possible destinations reachable from one SI. For example, the routes of w_2 and n_1 from I_0 are presented in Fig. 2 (dedicated left lane configurations). We rotate the same route patterns and apply them to the traffic arriving at all four SIs. Moreover, for each inflow lane, we generate the destinations randomly and uniformly among all seven possibilities.

Figure 3a presents the distance traveled by a vehicle crossing an arbitrary intersection I considering its maximum targeting speed (S_{max}), free flow speed (S_F), and the running speed (S_R). The figure also shows the three major delays that the vehicle suffers, namely the waiting time delay (WD), control delay (CD), and travel delay (TD). Travel delay is the difference between the target time and the actual time taken via the intersection. On the other hand, control delay is attributed to the IM operations at SIs and is part of the travel delay.

The waiting time delay, also called the stopped delay, occurs when a vehicle stops at the intersection entrance due to red signals (empty roads) or waiting in the queue (non-empty roads) to access the intersection. In Fig. 3a, this waiting time delay is shown in red color between t_2 (after deceleration) and t_3 (before acceleration); thus, the waiting time delay suffered by vehicle x at intersection I is $WD_{I(x)} = t_3 - t_2$. To characterize the intersection I, we compute the maximum waiting time delay over all vehicles that cross it ($WD_I = max_x(WD_{I(x)})$). We can also define the maximum waiting time delay along a specific route of intersections $\mathcal{I}$ as $WD_{\mathcal{I}} = \sum_{\forall I \in \mathcal{I}} WD_I$. Fig. 2 shows the routes of the dedicated left lane starting from inflow lanes w_2 and n_1 at intersection I_0. For the n_1 case, $\mathcal{I}_{n_1}$ may include I_0^R (turning right at I_0), I_0^L and $I_1^{L,S}$ (turning left at I_0 and then left or straight at I_1), I_0^S and $I_3^{R,S}$, or finally I_0^L, I_1^R and $I_2^{L,S}$. The corresponding maximum waiting time delay is given by Eq. 1.

As an illustration, when the vehicles arrive during the green phase (ϕ_g), they access the intersection without stopping. However, when they arrive during the end of the green phase or the beginning of the red phase (including the yellow phase), they must stop n TLC cycles from accessing the intersection.

$$WD_{\mathcal{I}_{n_1}} = \begin{cases} WD_{I_0^R}, & \text{if } \mathcal{I}_{n_1} = \{I_0\} \\ WD_{I_0^L} + WD_{I_1^{L,S}}, & \text{if } \mathcal{I}_{n_1} = \{I_0, I_1\} \\ WD_{I_0^S} + WD_{I_3^{R,S}}, & \text{if } \mathcal{I}_{n_1} = \{I_0, I_3\} \\ WD_{I_0^L} + WD_{I_1^R} + WD_{I_2^{L,S}}, & \text{if } \mathcal{I}_{n_1} = \{I_0, I_1, I_2\} \end{cases} \quad (1)$$

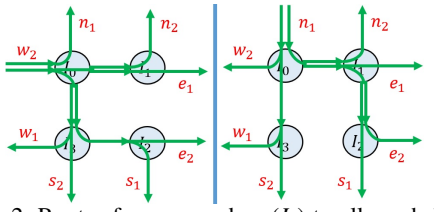

Fig. 2: Routes from w_2 and n_1 (I_0) to all reachable destinations (dedicated left-lanes).

The n TLC cycles depends on the maximum queue length (Q_{max}) and the number of vehicles ($D_{IM_{ij}}$) that the IM approach serves per road lane ij during the green phase. In practice, the maximum waiting delay ($WD_{IM_{ij}}$) depends on the specific inflow lane ij and the IM approach. Henceforth we will use the maximum waiting delay to characterize each IM approach on each type of lane for the considered intersections. We measure $WD_{IM_{ij}}$ per road lane ij at individual intersections by knowing the road capacity C (defined in section 3), traffic flow information, and IM-specific parameters. We use the Q_{max} that may build up in road lane ij (note that $Q_{max} \leq C$). The IM-specific parameters are the total (minimum or maximum) TLC cycle time ($T_{\Phi_{IM}}$), the minimum/maximum allocated green phase time (ϕ_g), and the maximum number of vehicles that the IM approach discharges during the green phase from each road lane ij ($D_{IM_{ij}}$). Equation 2 estimates the maximum waiting time delay at individual intersections.

$$WD_{IM_{ij}} = \begin{cases} T_{\Phi_{IM}} - \phi_g, & \text{if } Q_{max} \leq D_{IM_{ij}}; \\ (n-1) \times T_{\Phi_{IM}} + (T_{\Phi_{IM}} - \phi_g), & \text{if } D_{IM_{ij}} < Q_{max} \leq nD_{IM_{ij}}, \text{ where } n = \left\lceil \frac{Q_{max}}{D_{IM_{ij}}} \right\rceil. \end{cases} \quad (2)$$

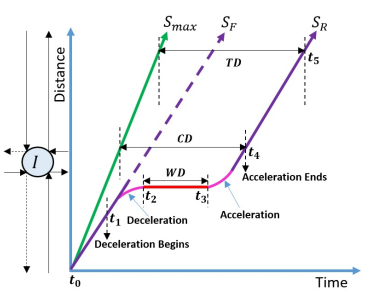

(a) Delays at signalized intersection I.

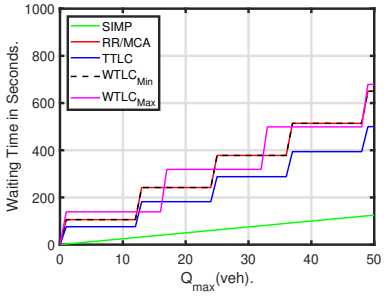

(b) Waiting time (s) on S/R lane.

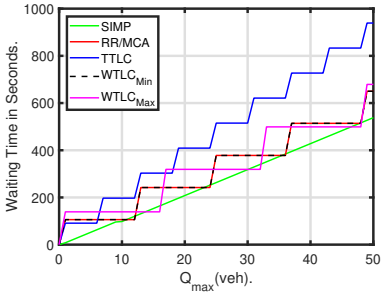

(c) Waiting time (s) on lane L.

Fig. 3: Various types of delays at each SI and waiting time delay (s) for various IM approaches with $C = 50$ on S/R- and L- lanes.

Fig. 3b and 3c present the maximum waiting time delays (s) of S/R ($j = 1$) and L ($j = 2$) lanes at a single intersection as a function of the maximum queue length, using Eq. 2. Index i refers to the two inflow lanes at each intersection (for I_0, we consider $i = n_1$ and w_2). We consider road lanes full capacity $C = 50$ (described in the following section) and the IM-specific parameters presented in Table 1. The results of Eq. 2 can then be used in Eq. 1 to compute the maximum waiting time delay for each concrete route. The step size in the traces in Figs. 3c and 3b depend on the number of vehicles that the IM approach serves during the green phase from each road lane, i.e., the higher green phase time leads to a bigger step size. From the graphs, it is clear that the lowest waiting time values are obtained with the SIMP protocol in both L and S/R lanes, and we represent it with a linear behavior because of its very short cycle time. Thus, the last (i.e., 50th) vehicle in the queue experiences maximum waiting delays. Conversely, for the other approaches, the first vehicle in every cycle undergoes maximum waiting delays as the following vehicles join the queue later. Among all IMs but SIMP, none dominates the other ones for the full range of possible Q_{max}. However, for $Q_{max} \geqslant 18$ vehicles, TTLC exhibits lower maximum waiting delays than the others in the S/R lanes, while it presents higher maximum waiting delays in the L lanes due to offering a lower service time. Note that the acyclic nature of MCA will adapt the green phase time dynamically based on the traffic flow movements. Thus, in Figs. 3c and 3b, we represent the worst-case behavior of this IM approach. For WTLC, we explicitly represent the service with the minimum and maximum cycle times. Finally, the value of Q_{max} depends on the interaction between the IM approach and the arrival pattern in each lane. The two possible ways of finding the Q_{max} are either measuring directly using road infrastructures or the distribution of traffic arrival patterns. In the analysis, we consider the Q_{max} values using the initial method while the work on the latter method is ongoing.

6. Simulation Settings

We designed two simulation scenarios to compare the waiting delay performance of five state-of-the-art IM approaches presented in section 4 (RR, TTLC, MCA, WTLC and SIMP). In **scenario-1**, all intersections are configured with dedicated left lanes while **Scenario-2** uses only shared left lanes. Note the IM approaches operate at individual SIs without coordination and cooperation. In both scenarios, the random injection of traffic on all external inflow lanes follows the *Poisson distribution*. A set of four average traffic arrival rates (0.025, 0.05, 0.067, and 0.1) in veh/s are used in sequence, each for $1h$; thus, the total simulated time is approximately $4h$. We simulate a long run until all the injected vehicles exit the road network. Once the last vehicle of the current arrival rate exits the grid network, then only the vehicles of the following arrival rate are injected. These rates cover from low to medium and near saturated traffic conditions. Note that this paper does not consider traffic saturation. The path of the injected vehicles follows predefined routes by picking them randomly and uniformly, as described in the previous section (Fig. 2).

The simulations were carried out with SUMO (v1.14.1 [16]) running on a computer with Intel Core-i5 8th generation, 8GB RAM and 64-bit Windows 11 OS. The geographic settings of the grid network are the following, road lane length of $500m$, intersection crossing space between $5m$ (right) and $20m$ (left), and the total grid side length of $D = 1540m$. Vehicles crossing one intersection travel at most $1020m$, two intersections $1540m$, and three intersections $2060m$. The average vehicle length is $5m$, and the average safety distance is $5m$, leading to a road lane capacity of $C = 50$. SUMO default values are employed for HVs and AVs, such as minimum time headway ($1s$) and driver imperfection (0.5 for HVs and 0 for AVs). We consider the injected traffic to be 50% HVs and 50% AVs. The maximum speed is $30km/h$ representing a low-speed urban environment. Other parameters include a maximum acceleration of $2.6m/s^2$, a maximum deceleration of $-4.5m/s^2$, and an emergency deceleration of $-9m/s^2$.

7. Results

This section presents the waiting time delays of the two scenarios with all vehicles grouped according to the number of intersections they crossed. We show both analytical (using Eqs. 1 and 2) and SUMO-provided waiting time results. For crossing a single intersection, our analysis provides a single value (marked with $\times$). However, for WTLC and MCA we provide two values (marked with $\times$ and $\times'$). These correspond to the minimum and maximum cycle times (WTLC) or an under or over-approximation of a cyclic behavior (MCA). When vehicles cross more than one intersection, Eq. 1 generates multiple results depending on the specific paths taken. We represent the lowest values obtained (marked with $\times$) and the highest ones (marked with a black +). For WTLC, we also represent the lowest value with the minimum cycle time (marked with $\times'$). Finally, we indicate the IM approaches with extension $* - D$ and $* - S$ for the dedicated (scenario-1) and shared (scenario-2) left lanes, respectively.

7.1. Scenario 1

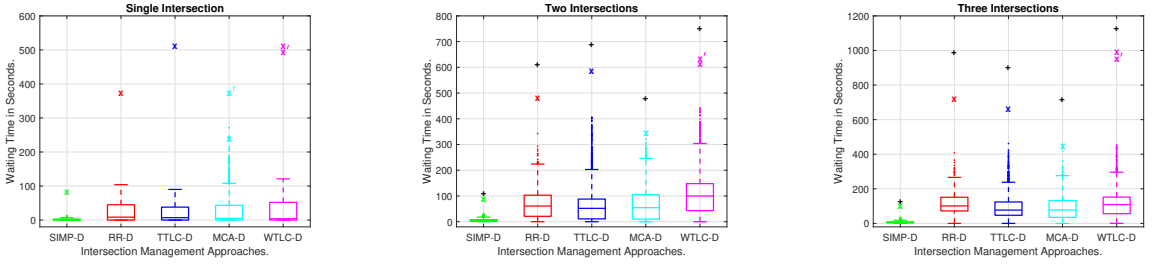

(a) Waiting Time (s) of 1039 vehicles. (b) Waiting Time (s) of 3993 vehicles. (c) Waiting Time (s) of 1948 vehicles.

Fig. 4: Waiting Time (s) of scenario-1 for 6980 vehicles crossing one (a), two (b) and three (c) intersections.

Figure 4 shows the waiting time delays of scenario-1 (dedicated left lane intersections). SIMP exhibits the lowest waiting time values (overall below $135s$), dominating all three cases in analytical and simulation results. The observed (simulation) values are significantly lower, though, showing pessimism in the analysis, which decreases for longer paths. The difference between analytical and maximum observed values for three intersections is below $20s$. The same pattern of higher pessimism of the analysis for single intersection paths, reducing for longer paths, is visible in all IM approaches. Due to its adaptive behavior, MCA shows a larger spreading of values in simulation with a single intersection (Fig. 4a). This case also shows that the analysis can be optimistic when under-approximating the cyclic behavior. The analysis always provided upper bounds for the observed waiting times for all other IMs.

Concerning the observed (simulation) results, SIMP stands out with significantly lower values and dispersion. The median value of SIMP in a single intersection (Fig. 4a) is $0s$, followed by WTLC with $4s$. When the vehicles cross two intersections (Fig. 4b), the median value of SIMP is $5s$, followed by TTLC with $52s$ (more than 10 times the median of SIMP). Crossing three intersections (Fig. 4c), SIMP median is $6s$, while the following best approaches are TTLC and MCA with $77s$ ($\sim$ 13 times more than that of SIMP). In all three cases, the worst-performing approaches are RR with $8.5s$ when crossing a single intersection and WTLC with $100s$ and $109s$ in the other two cases, respectively.

7.2. Scenario 2

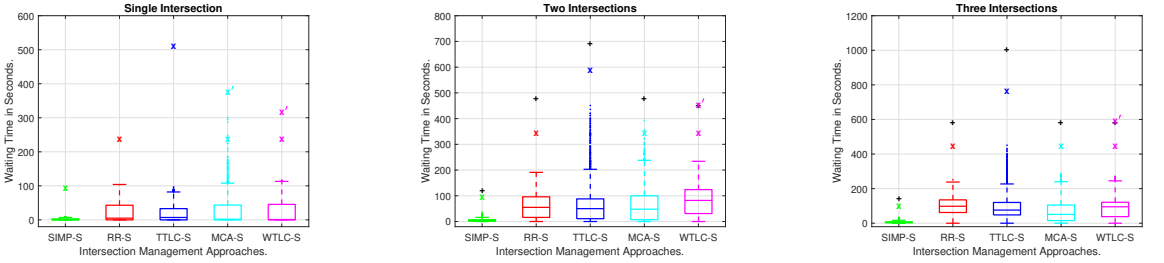

(a) Waiting Time (s) of 1039 vehicles. (b) Waiting Time (s) of 3993 vehicles. (c) Waiting Time (s) of 1948 vehicles.

Fig. 5: Waiting Time (s) of scenario-2 for 6980 vehicles crossing one (a), two (b) and three (c) intersections.

Fig. 5 shows the waiting time delays of scenario-2, i.e., when the intersections use shared left lanes. As the left lane is shared by the straight and left crossing vehicles, the queue lengths and associated waiting time delays are generally reduced. The analysis becomes, then, less pessimistic. We also see this pessimism reducing when the paths include more intersections. The only exception is TTLC. It has specific phases with shorter green time to handle left lanes, which are served simultaneously from opposite roads. In this case, a straight-crossing vehicle can block a left crossing one or vice versa. This leads to increased pessimism about the analysis (single intersection) and a higher spread of the waiting times with two and three intersections.

As in the previous scenario, SIMP is the best-performing approach with the lowest waiting time delays, followed by RR, WTLC and MCA, with TTLC being the worst due to the aspects just referred.

Concerning the distribution of the simulation results, SIMP is the best-performing approach in all three cases with median values of $0s$ (single intersection), $4s$ (two intersections), and $5s$ (three intersections), respectively, and very tight dispersion. The following best approaches are WTLC with $1s$ median (single intersection) and MCA with $48s$ and $51s$ median with two and three intersections. The worst performing ones are TTLC with $7s$, WTLC with 82, and RR with $98s$ medians for one, two, and three crossed intersections, respectively.

7.3. Discussions

The lowest waiting time delays of SIMP are due to the lowest control cycle time and the efficiency of using the CDM that allows synchronous access of one vehicle from each non-conflicting road lane. This aspect allows respecting the leader-follower driving control without hard braking or complete stops leading to very short (in fact, the shortest) queue lengths. Moreover, the queues on the left lanes grow more than those on the right lanes. Note the left lanes serve only one vehicle per cycle, while the S/R lanes serve multiple vehicles due to non-conflicting right crossings. The results indicate that SIMP maintains its efficiency even when operating in a grid network.

Conversely, the remaining IM approaches admit multiple consecutive vehicles from a single or multiple opposite lanes for longer green times, thus causing vehicles from other conflicting lanes to stop and wait until their turn. This behavior generates longer queues and waiting delays on red signals due to longer cycle times. We observed that RR and WTLC (dedicated left lane) showed longer queues on both external inflow and internal lanes forming the road network. For the same RR and WTLC (shared left lane), reduced queues are observed on all internal and external lanes due to the sharing of straight-crossing vehicles among the S/R and L lanes. Differently, both dedicated and shared left lane intersections of TTLC showed longer queues on particular external inflow lanes (n_2, e_2, s_2, w_2), while all other lanes showed shorter queues. In the case of MCA-D, only the external inflow lanes showed longer queues. In contrast, the internal lanes interestingly showed the same maximum queue lengths leading to the same waiting time delays. Reduced queue lengths are observed with the MCA-S, similar to RR-S and WTLC-S.

For all IM approaches, we compared the observed waiting time delays against the analytical ones, giving a perception of the pessimism of the analysis. Except for MCA, for which case the analysis is not totally accurate, the obtained values were always above the ones observed in simulation, validating the worst-case character of the analysis. Curiously, the pessimism was relatively higher for paths with a single intersection than with more intersections.

8. Conclusions & Future Work

In this paper, we presented an analytical expression for estimating the maximum waiting time delays of vehicles crossing a set of SIs. We considered a concrete case of a 2×2 grid network of complex intersections, each with four legs and two lanes, with both dedicated and shared left lanes. We compared the performance of this network when using five state-of-the-art IM approaches applied independently at each intersection, namely RR, TTLC, MCA, WTLC and SIMP. The comparison included two simulation scenarios, one for dedicated and another one for shared left lanes. The simulations were carried out in SUMO under varying traffic arrival rates below saturation conditions. The observed waiting time results validate the analytical values and show the dominance of the SIMP protocol in the tested scenarios. In future work, we will design and analyze various traffic scenarios with arbitrary road networks and events in the network, e.g., emergency vehicles, accidents and roadblocks.

Acknowledgements

This work was supported by FCT/MCTES (Portuguese Foundation for Science and Technology) under grant UIDP/UIDB/04234/2020 (CISTER unit); by FCT through the European Social Fund (ESF) and the Regional Operational Programme NORTE2020, under grants 2021.05004.BD, POCI-01-0247-FEDER-045912 (FLOYD) and NORTE-01-0145-FEDER-000062 (RETINA); and by FCT and EU ECSEL JU within ECSEL/0010/2019 - JU grant nr. 876019 (ADACORSA) - The JU receives support from the European Union's Horizon 2020 research and innovation programme and Germany, Netherlands, Austria, France, Sweden, Cyprus, Greece, Lithuania, Portugal, Italy, Finland, Turkey (Disclaimer: This document reflects only the author's view and the Commission is not responsible for any use that may be made of the information it contains).

References

[1] Björck, Erik, and Fredrik Omstedt., 2018. A comparison of algorithms used in traffic control systems. School of Electrical Engineering and Computer Science, Stockholm, Sweden, pp.1-38.

[2] Boon, M.A. and van Leeuwaarden, J.S., 2018. Networks of fixed-cycle intersections. Transportation Research Part B: Methodological, 117, pp.254-271.

[3] Varaiya, P., 2013. Max pressure control of a network of signalized intersections. Transportation Research Part C: Emerging Technologies, 36, pp.177-195.

[4] Webster, F. V. (1958). Traffic Signal Settings. Road Research Laboratory Technical Paper No. 39, HMSO, London.

[5] Tlig, M., Buffet, O. and Simonin, O., 2014, May. Decentralized traffic management: A synchronization-based intersection control. In 2014 IEEE International Conference on Advanced Logistics and Transport (ICALT), pp.109-114.

[6] Reddy, R., Almeida, L. and Tovar, E., 2019, December. Work-in-Progress: Synchronous Intersection Management Protocol for Mixed Traffic Flows. In 2019 IEEE Real-Time Systems Symposium (RTSS), pp.576-579.

[7] Reddy, R., Almeida, L., Gaitán, M.G., Santos, P.M. and Tovar, E., 2021, September. Synchronous Framework Extended for Complex Intersections. In 24th Euro Working Group on Transportation Meeting, pp.1-3.

[8] Eom, M. and Kim, B.I., 2020. The traffic signal control problem for intersections: a review. European transport research review, 12(1), pp.1-20.

[9] Dowling, R., 2007. Traffic analysis toolbox volume vi: Definition, interpretation, and calculation of traffic analysis tools measures of effectiveness (No. FHWA-HOP-08-054). United States. Federal Highway Administration. Office of Operations.

[10] Olszewski, P., 1993. Overall delay, stopped delay, and stops at signalized intersections. Journal of transportation engineering, 119(6), 835-852.

[11] Othayoth, D. and Rao, K.K., 2020. Assessing the relationship between perceived waiting time and level of service at signalized intersection under heterogeneous traffic conditions. Asian Transport Studies, 6, p.100024, pp.1-7.

[12] Chandra, S., Gangopadhyay, S., Velmurugan, S. and Ravinder, K., 2017. Indian highway capacity manual (Indo-HCM).

[13] Wu, X., Levinson, D.M. and Liu, H.X., 2009. Perception of waiting time at signalized intersections. Transportation research record, 2135(1), pp.52-59.

[14] Reddy, R., Almeida, L., Santos, P.M. and Tovar, E. Work-in-Progress: Exploring the Composition of Synchronous Intelligent Intersections, In 43rd IEEE Real-Time Systems Symposium (RTSS), 2022, pp.523-526.

[15] Chandler, B.E., Myers, M., Atkinson, J.E., Bryer, T., Retting, R., Smithline, J., Trim, J., Wojtkiewicz, P., Thomas, G.B., Venglar, S.P. and Sunkari, S.R., 2013. Signalized intersections informational guide (No. FHWA-SA-13-027). United States. Federal Highway Administration.

[16] Lopez, P.A., Behrisch, M., Bieker-Walz, L., Erdmann, J., Flötteröd, Y.P., Hilbrich, R., Lücken, L., Rummel, J., Wagner, P. and Wießner, E., 2018, November. Microscopic traffic simulation using sumo. In 2018 21st IEEE International Conference on Intelligent Transportation Systems (ITSC), pp.2575-2582.